ELSEVIER

Journal of Power Sources 81–82 (1999) 39–43

JOURNAL OF POWER SOURCES

www.elsevier.com/locate/jpowsour

Enhancement of the electrochemical properties of $Li_1Mn_2O_4$ through chemical substitution

G.G. Amatucci [a,*], N. Pereira [a,b], T. Zheng [a], I. Plitz [a], J.M. Tarascon [c]

[a] *Bellcore, Energy Storage Research Group, 331 Newman Springs Road, Red Bank, NJ 07701, USA*
[b] *Rutgers University, Piscataway, NJ 08855, USA*
[c] *Universite de Picardie Jules Verne, Amiens 80000, France*

Abstract

The link between room temperature (RT) cycling failure for $Li_1Mn_2O_4$-type spinels and elevated temperature (ET) failure of $Li_{1.05}Mn_{1.95}O_4$ materials was investigated by physical and electrochemical characterization. Failure for both ET and RT cycling occurred at the end of discharge. Substantial evidence suggesting a link based on the cooperative Jahn–Teller distortion was found. Based on this knowledge, $LiAl_xMn_{2-x}O_{4-\delta}F_z$ materials were fabricated. These novel compounds were found to offer much improved capacity and ET performance than present generation materials. Three hundred cycles at 55°C resulted in 15% capacity loss. Storage in charged and discharged state for 4 days at 70°C revealed less than 1.6% irreversible capacity loss.

Keywords: $Li_1Mn_2O_4$; Jahn–Teller distortion; Chemical substitution

1. Introduction

Li-ion battery technology has been enjoying a significant commercial success addressing the power demands of wireless communications and portable computing mainly due to high energy density, long life, and safety. The technology is rapidly approaching the time when it will be the powering solution for larger applications such as electric bicycles, scooters, wheelchairs, and possibly even cars and trucks. For such an evolution to occur successfully, the cost and safety of the Li-ion cell will become issues of paramount importance. A major factor contributing to the cost of present day lithium ion cell is the use of $LiCoO_2$ as the positive electrode [1]. Even as $LiCoO_2$ is replaced with the less expensive, higher capacity $LiCo_xNi_{1-x}O_2$, the cost of such cells will still remain high. The $LiMn_2O_4$ spinel, although having less reversible capacity than the others, offers an alternative with a cost approximately 5–6 times cheaper than $LiCoO_2$ and 2–3 times cheaper than $LiCo_xNi_{1-x}O_2$ [2]. Before the spinel can be successfully implemented into Li-ion batteries on a commercial basis, all performance issues with respect to lifetime must be on par with the OEM accepted $LiCoO_2$.

Early in its introduction, $LiMn_2O_4$ suffered from poor cycling efficiency at room temperature (RT). After a an extensive research effort, it was found that monovalent, divalent, or trivalent cationic substitutions for the manganese improved RT performance to where over 2000 cycles could be made before end of life [3,4]. The improvement is attributed to the increase in the average oxidation state of the manganese [5]. Since then, a large number of papers and patents have been published regarding these cationic substitutions.

The remaining performance issue regarding the acceptance of the spinel into the commercial arena is performance at elevated temperatures (ETs). At temperatures exceeding 45°C the spinel suffers from irreversible capacity loss in storage and cycling. Initial publications with respect to the failure mechanism focused on manganese dissolution rooted in the disproportionation of Mn^{3+}. Recently, however, the mechanism has been extended to the ion exchange of H for Li within the tetrahedral 8a and octahedral 16d sites. The source of H is found in the always present quantities of HF in the electrolyte, either from initial contamination or formed by products of side reactions involving the cell components and the electrolyte [6–8].

We have proposed a number of ways to improve the ET performance of the spinel ranging from focus on the

* Corresponding author. Tel.: +1-732-758-3358; Fax: +1-732-758-4372; E-mail: gga@cc.bellcore.com

0378-7753/99/$ - see front matter
PII: S0378-7753(99)00186-X

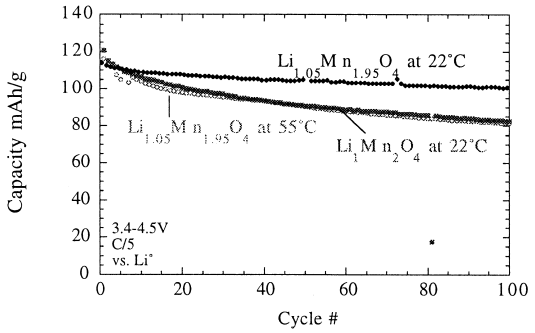

Fig. 1. Comparison of cycle life of $LiMn_2O_4$ (22°C) and $Li_{1.05}Mn_{1.95}O_4$ (22°C and 55°C).

fabrication of low surface area spinels to introduction of an encapsulation concept where the surface of the spinel is removed from contact with HF containing electrolyte [9]. All of these have been shown to improve to a degree the ET properties of the spinel. However, to date, none bring the ET performance of the spinel to an acceptable level in a practical manner.

Recently, we have shown that the introduction of anion substitution in the form of spinel oxyfluorides ($Li_{1+x}Mn_{2-x}O_{4-z}F_z$) improves the ET storage performance of the spinel. Although the presence of fluorine within the structure improves the ET storage of the spinel, it was found to have surprisingly little effect on the cycle life at ETs, with the spinel failing at a rate of approximately 20–25% after 100 cycles at 55°C. The paradox of improved storage properties but poor cycle life at ET required re-analysis of he interaction of the failure mechanism involved in order to design a spinel of improved ET properties. For the past 4 years, investigation into improved ET performance has been decoupled from the poor cyclability of $Li_1Mn_2O_4$ at RT. In this paper we introduce a link between the two mechanisms and offer a possible solution to the ET failure in the form of $Li_{1+x}Al_y$-$Mn_{2-x-y}O_{4-\delta}F_z$ solid solutions.

2. Experimental

$Li_{1+x}Mn_{2-x}O_4$ and $Li_{1+x}Al_yMn_{2-x-y}O_{4-\delta}F_z$ were prepared by intimate mixing of Li_2CO_3, LiF, MnO_2, and Al_2O_3 in stoichiometric quantities. Samples were annealed in air at 800°C. Experimental evidence not presented here suggests δ exceeds z and a degree of anion defects occurs within the anion sublattice. Positive electrodes were prepared by mixing 85% active material with 5% polyvinylidene fluoride binder (Aldrich) and 10% Super P carbon black (MMM). Five hundred milligrams of active material solution were mixed for 10 h in approximately 1 cm^3 *N*-methyl-pyrrolidinone. The solution was then cast on aluminum foil and dried for 1 h at 100°C. Electrodes were punched into 1 cm^2 disks. Swagelok™ cells were fabricated in the following configuration: Al plunger, positive electrode disk, Whatman GF/D glass fiber separator paper, Li metal, Ni disk, stainless plunger. The cell was filled with 1 M $LiPF_6$ 2EC:DMC electrolyte (v/v), the entire assembly was sealed in a He filled glovebox (−80°C dew point) and cycled in a dry room using a MacPile galvanostat cycler. All cycling was performed at constant current within the rates and voltage cutoffs described in text. X-ray diffraction was performed in a Scintag PADV diffractometer using Cu Kα radiation.

3. Results

As expected, the incorporation of $Li_{1+x}Mn_{2-x}O_4$ compositions improves the RT cycle life of the $Li_1Mn_2O_4$ compositions (Fig. 1). The capacity fade at 55°C for $Li_{1+x}Mn_{2-x}O_4$ composition was found to have an identical signature of the RT fade of the $Li_1Mn_2O_4$ compositions (Fig. 1) The similarity suggests a link between the ET failure mechanism of stabilized spinels $Li_{1+x}Mn_{2-x}O_4$ and the RT failure mechanism of stoichiometric $Li_1Mn_2O_4$. As $Li_{1.05}Mn_{1.95}O_4$ at 55°C fails similarly to $Li_1Mn_2O_4$, the same mechanism should follow such that $Li_1Mn_2O_4$ at low temperature should cycle as well as $Li_{1.05}Mn_{1.95}O_4$ at RT. Fig. 2 indeed shows that this is the case, supporting the theory that the RT failure mechanisms for $Li_1Mn_2O_4$ type spinels are related to the ET mechanisms for $LiM_xMn_{2-x}O_4$ type spinels.

The basis for the capacity loss at RT was investigated through the use of $Li_{1+x}Mn_{2-x}O_4$ compositions. Spinels of lower average oxidation state (larger lattice parameter) always incur a greater capacity difference between the first charge and discharge when cycling at RT. In order to examine this relationship, samples of differing average oxidation state were fabricated by varying the x in $Li_{1+x}Mn_{2-x}O_4$, these samples were charged and discharged at C/5 between 3.4 and 4.5 V. The change in average oxidation state of the Mn cation was traced through measurement of coulombs passed. A graph incorporating the average oxidation state at the end of charge and the end of discharge is presented in Fig. 3. From this plot it is

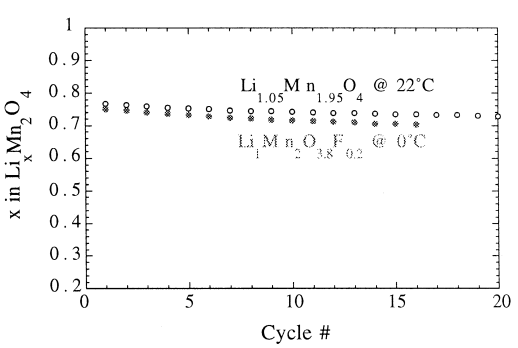

Fig. 2. Comparison of cycle life of $LiMn_2O_4$ type spinel ($LiMn_2O_{3.8}F_{0.2}$) at 0°C and $Li_{1.05}Mn_{1.95}O_4$ at 22°C.

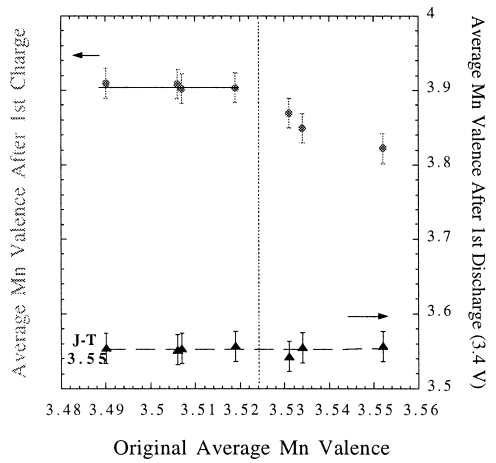

Fig. 3. Average Mn oxidation state as a function of charge.

apparent that all samples reach the end of discharge at an average oxidation state of 3.55, regardless of the initial sample average oxidation state. The difference between the initial and final oxidation state is the capacity difference between the first charge and discharge which worsens for samples of lower average oxidation states. A uniform end of discharge average oxidation state is consistent with a critical concentration of Mn^{3+} required to induce a cooperative Jahn–Teller distortion and formation of $Li_2Mn_2O_4$ on the spinel surface.

Fig. 4 shows the relationship between percent capacity loss after 25 cycles at RT and the average manganese oxidation state. The percent irreversible capacity loss at RT scales sharply with initial average oxidation state and then tends to level off for average Mn valence states greater than 3.55, the exact number calculated as the onset of the cooperative Jahn–Teller distortion in Fig. 3. The average oxidation state scales with lattice parameter due to the small size difference between Mn^{3+} (0.66 Å) and Mn^{4+} (0.60 Å). Fig. 5 plots the percentage capacity loss at RT and the initial lattice parameter, a nonlinearity is found as in Fig. 4. The lattice parameter at the nonlinearity is approximately 8.23 Å, this value coincides well with that found by Tarascon et al. [4] for the fabrication of spinels

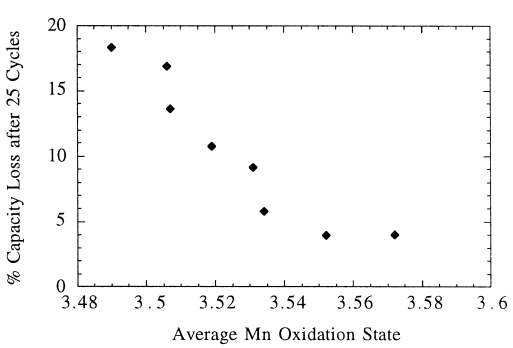

Fig. 4. Percent capacity loss after 25 cycles as a function of initial average oxidation state.

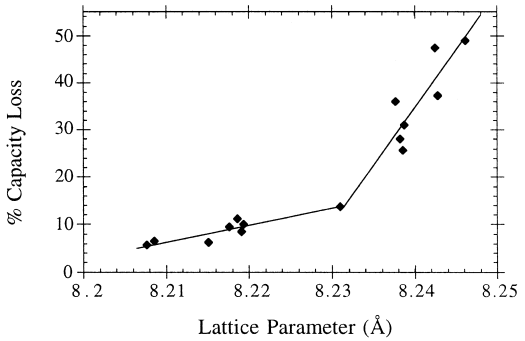

Fig. 5. Percent capacity loss after 25 cycles as a function of initial lattice parameter.

which cycle well at RT. As lithium is removed from the $Li_1Mn_2O_4$ spinel, the lattice parameter shrinks and the average oxidation state increases. Therefore, if the average oxidation state/lattice parameter upon discharge is the only parameter necessary to improve the RT cycle life, limiting the discharge to a smaller lattice parameter/higher average oxidation state during discharge should improve cyclability. An easy way to limit the amount of lithium re-inserted into the spinel, besides modification of the discharge voltage, is to fabricate a Li-ion battery.

During the first discharge in a Li-ion battery, the 20% irreversible capacity loss associated with the formation of the SEI layer on the coke does not allow full re-intercalation of lithium into the manganese spinel, therefore, the end of discharge occurs at a lattice parameter of 8.21 Å instead of the original 8.247 Å, well within the good cycling region established in Fig. 4. The spinel used in this experiment is $Li_1Mn_2O_4$, therefore, it is expected to have a poor cyclability vs. lithium metal shown in Fig. 6. When the discharge is limited by the use of the rocking chair battery, we see that the cyclability of the spinel improves significantly. Similar to the RT experiment, relithiation was limited for $Li_{1.05}Mn_{1.95}O_4$ by limiting discharge cutoff to 3.4, 3.9, or 4.0 V except cycling was performed at 55°C. A substantial improvement in cyclability was noted for the cutoff at 4.0 V (Fig. 7), supporting the conclusion that the ET failure occurs during discharge as observed at 22°C.

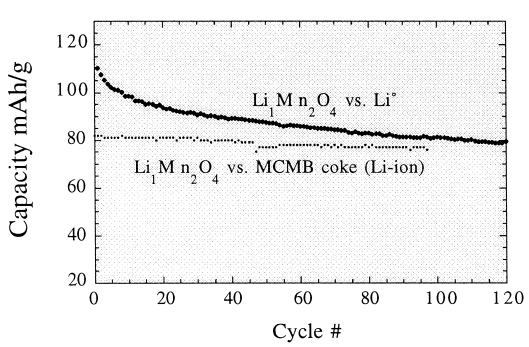

Fig. 6. Cycle life comparison of $Li_1Mn_2O_4$ cycled vs. coke and Li metal.

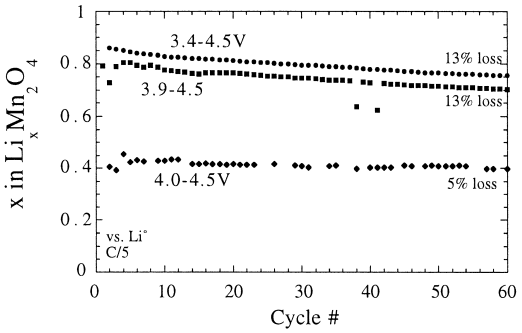

Fig. 7. Comparison of cycle life at 55°C for $Li_{1.05}Mn_{1.95}O_4$ discharged to 3.4, 3.9 and 4.0 V.

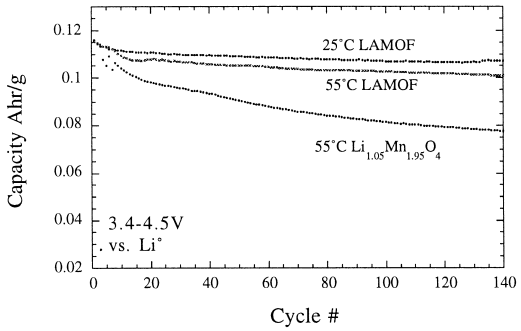

Fig. 9. Cycle life comparison of $Li_{1.05}Mn_{1.95}O_4$ (55°C) and $LiAl_{0.2}Mn_{1.8}O_{4-\delta}F_z$ (22°C and 55°C).

The results presented above suggest elimination of any trace of gradient-induced cooperative Jahn–Teller distortion will be effective in improving the capacity retention at 55°C. Based on the fundamentals of the cooperative Jahn–Teller distortion, Al^{3+} was chosen to substitute Mn on the 16d sites. Aluminum has a small ionic size, 0.53 Å. The small size restricts the dynamic Jahn–Teller Mn^{3+} cations from forming a cooperative c/a expansion. Aluminum is light weight, therefore improving specific capacity. The aluminum cation is trivalent allowing greater substitution than Li^+ on the 16d sites while retaining Mn^{3+} content critical for retention of capacity. Aluminum is extremely stable in an octahedral environment and will allow the maximization of substitution.

$LiAl_{0.1}Mn_{1.9}O_4$ and $LiAl_{0.2}Mn_{1.8}O_4$ were fabricated and cycled at 55°C for 150 cycles, 24% and 16% capacity fade was recorded, respectively. The much improved $LiAl_{0.2}Mn_{1.8}O_4$ exhibited a low capacity (on the order of 90 mA h/g), too low for practical use in Li-ion technology.

It was shown in our previous paper that the use of monovalent fluorine substitution for divalent oxygen increases the amount of Mn^{3+} content available for redox (thereby increasing specific capacity) with little penalty in capacity fading. Compositions of $LiAl_xMn_{2-x}O_{4-\delta}F_z$ (LAMOF) were fabricated with various F substitution. The *a* lattice parameter was found to increase with fluorine quantity for all *x* values. The trend is opposite to what is expected by Vegard's rule for the substitution of O for the smaller F anion. Therefore, the increase in lattice parameter can be assumed to originate in the increase in quantity of the larger trivalent manganese due to the successful reduction of Mn^{4+} by monovalent fluorine. F substitution resulted in the systematic increase in capacity for samples as a function of *z*. $LiAl_{0.2}Mn_{1.8}O_{4-\delta}F_z$ sample exhibited a 17% increase in capacity with respect to the pure oxide while retaining excellent 55°C performance (Fig. 8).

Fig. 9 compares the cycle life of $LiAl_{0.2}Mn_{1.8}O_{4-\delta}F_{0.5}$ at RT and 55°C with respect to the standard spinel oxide $Li_{1.05}Mn_{1.95}O_4$ at 55°C. The difference in 55°C capacity retention between the LAMOF sample and pure oxide is dramatic. In addition, there is very little difference between the RT and 55°C cycle fade for the LAMOF sample. Extended cycling at a rate of C/5 for 300 cycles at 55°C resulted in approximately 15% capacity loss.

LAMOF samples were tested for their ET storage performance in coin cells. Samples were cycled between 3.4 and 4.5 V at RT for approximately 10 cycles. The samples were then stored in their charged or discharged state at 70°C for 4 days, after which the samples were removed and started on cycle at RT on charge or discharge, respectively. In the charged state a reversible capacity loss was observed due to self-discharge in the charged state, but almost all capacity was recovered on the following cycle and less than 1% irreversible capacity loss was measured.

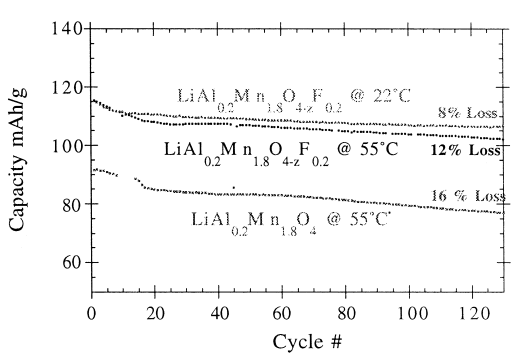

Fig. 8. Comparison of cycle life of $Li_1Al_{0.2}Mn_{1.8}O_4$ and $LiAl_{0.2}Mn_{1.8}O_{4-\delta}F_z$.

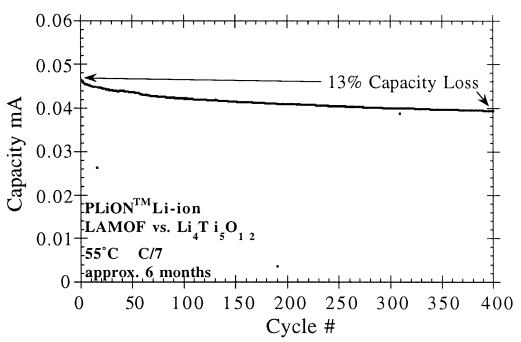

Fig. 10. Cycle life of Li-ion (PLiON™) cells incorporating $LiAl_{0.2}Mn_{1.8}O_{4-\delta}F_z$ as a positive electrode and $Li_4Ti_5O_{12}$ as negative electrodes.

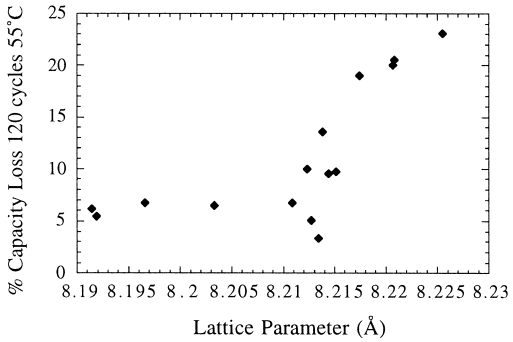

Fig. 11. Percent capacity loss after 120 cycles at 55°C as a function of initial lattice parameter.

In the discharged state, a capacity gain was found, this can be traced to self-discharge in the discharge state where lithium from the lithium anode is inserted into the 3 V plateau. The following cycles at 3.4 V cutoff reveal that also in the discharged state, less than 1.5% irreversible capacity loss was observed after 4 days at 70°C. Initial LAMOF spinels were fabricated into Li-ion (PLiON™) cells using the $Li_4Ti_5O_{12}$ as a stable baseline anode material. Capacity loss of 13% were measured after 400 cycles at 55°C (6 months) (Fig. 10).

Recent optimization of LAMOF materials resulted in first charge capacities exceeding 140 mA h/g while retaining capacity at ETs.

4. Discussion

Percent capacity loss after 120 cycles at 55°C is plotted as a function of lattice parameter in Fig. 11 for samples of $Li_{1+x}Mn_{2-x}O_{4-\delta}F_z$, $LiAl_xMn_{2-x}O_{4-\delta}F_z$, and $LiMg_xMn_{2-x}O_{4-\delta}F_z$. Capacity loss as little as 5% was observed. The same nonlinearity is noted as was observed at RT in Fig. 5, further establishing the link between RT and ET failure mechanisms. The difference between the two plots is nestled in the shift of the nonlinearity point from 8.23 Å (RT) to 8.21 Å (55°C). Therefore, the stability region for ET properties is for a spinel with a lattice parameter below 8.21 Å. Typical samples of $LiAl_{0.2}Mn_{1.8}O_{4-z}F_{0.2}$ presented in the text has lattice parameters below 8.215 Å.

The data presented in this paper clearly supports a link between the RT and ET failure mechanisms based on the cooperative Jahn–Teller distortion. During discharge at moderate rates, it is likely that the surface may have a local gradient of Li concentration, resulting in $Li_2Mn_2O_4$ Jahn–Teller distorted phase. The large lattice parameter differential results in surface cracking and pitting. The combination of increased surface area and the formation of Mn^{3+} rich $Li_2Mn_2O_4$ on the surface makes the material highly susceptible to Mn^{2+} dissolution through the disproportionation of $2Mn^{3+}$ to Mn^{4+} and Mn^{2+}. The Mn^{4+} rich distorted surface phase can the be attacked by mechanisms outlined by Ammundsun and Tarascon. In addition, it should be noted that the $LiAl_{0.2}Mn_{1.8}O_{4-\delta}F_z$ have no Li on the 16d sites which decreases susceptibility to H ion exchange. The difference in a sample's susceptibility to the ET failure mechanisms at all temperatures is rooted in the degree to which the spinel is subjected to the gradient induced distortions (a function of Mn^{3+} content and lattice parameter). This is the mechanism by which the spinels differ in performance upon cycling. The degree of capacity loss scales with temperature for all samples, this can be attributed to the kinetics involved in the 'high temperature' failure mechanisms (Mn^{3+} disproportionation, H exchange) outlined in literature. It can be expected that the performance of all spinels will shifted in unison by traditional means such as lowering of HF content present in the activated battery.

5. Conclusion

Preliminary investigations revealed evidence for a mechanistic link between the ET failure mechanisms of $Li_{1+x}Mn_{2-x}O_4$ spinels and the RT failure of $Li_1Mn_2O_4$ spinels. Failure mechanisms upon cycling were found to occur at the end of discharge at both RT and ET. With respect to this link, a new spinel, $Li_{1+x}Al_y$-$Mn_{2-x-y}O_{4-\delta}F_z$ was introduced which exhibits elevated temperature performance competitive with $LiCoO_2$.

References

[1] T. Nagaura, T. Tazawa, Prog. Batteries Sol. Cells 9 (1990) 20.
[2] T. Ohzuku, A. Ueda, M. Nagayama, Y. Iwakoshi, H. Komori, Electrochim. Acta 38 (1993) 1159–1167.
[3] R.J. Gummow, A. de Kock, M.M. Thackery, Solid State Ionics 69 (1994) 59.
[4] J.M. Tarascon, W.R. McKinnon, F. Coowar, T.N. Bowmer, G. Amatucci, D. Guyomard, J. Electrochem. Soc. 141 (1994) 1421.
[5] M. Thackery, Y. Shao-Horn, A. Kahaian, K. Kepler, E. Skinnwer, J. Vaughey, S. Hackney, Electrochem. Solid State Lett. 1 (1998) 7.
[6] B. Ammundsen, D.J. Jones, Roziere, Chem. Mater. 7 (1995) 2151.
[7] B. Ammundsen, P.B. Aitchinson, G.R. Buruns, D.J. Jones, J. Roziere, Solid State Ionics 97 (1997) 3342.
[8] A. du Pasquier, A. Blyr, A. Cressent, C. Lenain, G. Amatucci, J.M. Tarascon, Solid State Ionics.
[9] G.G. Amatucci, A. Blyr, C. Sigala, P. Alfonse, J.M. Tarascon, Solid State Ionics 104 (1997) 13–25.